Tracking Aggregate Active- and Reactive-power Setpoints for a Collection of Dispatchable Inverters

Abdullah Al-Digs[§], Victor Purba[†], Sairaj V. Dhople[†], and Yu Christine Chen[§]
[§]The University of British Columbia. E-mails:{aldigs, chen}@ece.ubc.ca
[†]University of Minnesota. E-mails:{purba002, sdhople}@umn.edu

***Abstract*—This paper proposes a strategy to regulate active- and reactive-power injections of a collection of dispatchable inverters so that the distribution feeder where they are installed can, in aggregate, track active- and reactive-power regulation signals issued by a higher-level aggregator. At its core, the proposed method relies on the linear mapping of nodal active- and reactive-power injections to the active and reactive power injected into the bulk transmission grid and a linear-quadratic-regulator (LQR) controller. We demonstrate the effectiveness of the proposed LQR controller using regulation signals from Pennsylvania-New Jersey-Maryland Interconnection (PJM) for a collection of 15 inverters (each with a 15th-order model capturing phase locked loop, LCL filter, power- and current-controller dynamics) installed in a modified IEEE 37-bus distribution feeder. We also evaluate the ability of the proposed controller to track regulation signals with different sampling and dispatch rates.**

I. Introduction

The increase in behind-the-meter integration of inverter-interfaced electrical vehicles, photovoltaic systems, and energy-storage devices offers tremendous potential to provide essential ancillary services required to operate the bulk power system reliably [1]. Given the sheer number of dispatchable inverters expected to be commonplace in the future system, there is a pressing need to develop strategies to operate them at scale. This involves developing sensing and control architectures to steer the collective dynamic behaviour of ensembles of dispatchable distributed energy resources (DERs). Such controllable collections of DERs have come to be known as *virtual power plants* (VPPs).

There is a wide body of existing work to realize and optimize the operation of VPPs. Tailored solutions for electric vehicles, thermostatically controlled loads, building HVAC systems, energy-storage devices, and photovoltaic energy conversion systems have been developed and demonstrated at various levels of technology readiness [2]–[6]. More generally, theory and algorithms for management of DERs have included: development of synthetic droop and inertia controllers and setpoint optimization to respond to frequency events precipitated from the bulk power system [7]–[9], following regulation signals issued by aggregators that manage VPPs [10], [11], regulating system voltage by controlling reactive power of the DERs [12], [13], and optimizing distribution-network power quality [14], [15]. In this work, we focus on the problem of following regulation signals and propose an approach that makes several contributions over the state-of-the-art (see Fig. 1 for an illustration). First, a linear-quadratic-regulator (LQR) controller is synthesized while leveraging linear sensitivities of the power flow at the feeder head where regulation is desired (marked "Sensitivities" in Fig. 1) to the power injections at inverter buses. As a direct consequence, the resulting controller innately embeds network attributes via sensitivities of nodal power injections on feeder-head power flow. Furthermore, the controller acknowledges power ratings of the inverters, i.e., the power provided by inverters to meet the feeder-head requirement is in proportion to their power ratings. Finally, the controller utilizes both active- and reactive-power injections ($\Delta P^\star$ and $\Delta Q^\star$) to track active- and reactive-power reference trajectories, ($P^\star_{\text{grid}}$ and $Q^\star_{\text{grid}}$), issued by the VPP aggregator. In our simulations, we track the PJM dynamic regulation (regD) trajectory [16] with sampling (for P_{grid} and Q_{grid}) and relay (for $\Delta P^\star$ and $\Delta Q^\star$) rates of 0.001 sec, 0.01 sec, and 0.05 sec. We validate the proposed strategy with time-domain simulations involving a nonlinear 15th-order inverter model that includes dynamics arising from output filters, phase-locked loops, and current and power controllers. Simulations are performed for a system with 15 inverters installed at arbitrary locations in a modified IEEE 37-bus

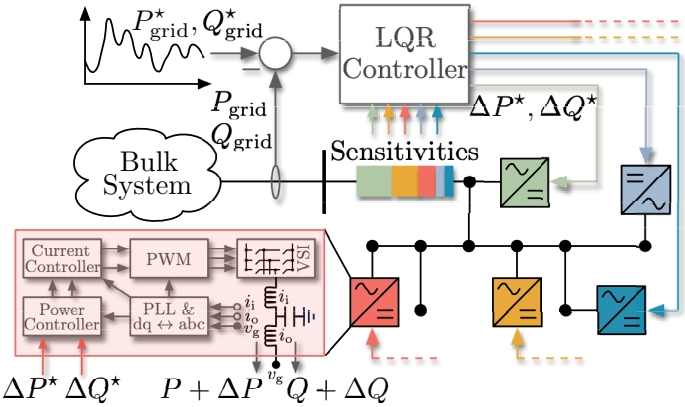

Fig. 1: Control architecture modulates setpoints $\Delta P^\star$ and $\Delta Q^\star$ for a collection of inverters so that the distribution feeder acts as a virtual power plant and tracks feeder-head active- and reactive-power references $P^\star_{\text{grid}}$, $Q^\star_{\text{grid}}$. Inset depicts block diagram of inverter-control loops.

Funding support from the Natural Sciences and Engineering Research Council of Canada (NSERC), funding reference numbers RGPIN-2016-04271 and PGSD3-519078-2018, and from the National Science Foundation (NSF) through grant ECCS-1453921 is greatly appreciated.

978-1-7281-1842-0/19/$31.00

feeder. This last aspect is central to demonstrate the viability of the proposed architecture as it establishes feasibility while acknowledging the admittedly complex dynamical behaviour of power-electronic inverters, a point that is often approximated or entirely overlooked in related prior art. Finally, we mention that the method proposed in this work builds off our previous effort [17] that was tailored to control of transmission-line flows in the bulk power system. (We also refer readers to [17] for other related work in the general domain of control of line flows.)

The remainder of this paper is organized as follows. In Section II, we describe the system and pertinent dynamical models. Section III outlines design aspects of the LQR controller to achieve optimal tracking of active- and reactive-power grid injections. In Section IV, we demonstrate the utility of the controller via case studies involving the IEEE 37-bus distribution feeder. Finally, concluding remarks and directions for future work are provided in Section V.

II. System Dynamical Model

In this section, we briefly describe the inverter dynamical model. Following this, using a linear mapping of nodal injections to the power flow at the feeder, we develop a discrete-time system model that is suitable for control synthesis.

A. Inverter Dynamics

A block diagram of the inverter is depicted in the inset in Fig. 1. The physical side consists of a full bridge voltage source inverter (VSI) and an output LCL filter. All controllers are realized in their local dq reference frame, and the controllers include: an outer-loop power controller, an inner-loop current controller, a pulse-width modulation (PWM) block, and a phase-locked loop (PLL). The power controller tracks active- and reactive-power setpoints and generates current references to the current controller. (This is an abstraction for the DC-side dynamics that we do not explicitly model.) It consists of two PI controllers and low pass filters. The current controller consists of two PI loops, and it generates the terminal voltage references for the PWM block, which subsequently provides switching signals. In our implementation, the PLL consists of a PI controller and a low-pass filter, and it synchronizes with the grid by modulating the PLL angle such that the d-component of the inverter bus voltage is driven to 0. The inverter dynamical model is order 15 and full details are available in [18].

For the purpose of this paper, we will assume that inverter input references $P^\star$, $Q^\star$ are pre-determined in a decentralized manner based on some local controller (e.g., a maximum power point tracking routine) and the physcially realized outputs of the inverter at the LCL filter terminals are denoted by P, Q. Our proposed LQR controller dictates changes to the input references $\Delta P^\star$, $\Delta Q^\star$, such that the modulated reference setpoints $P^\star + \Delta P^\star$, $Q^\star + \Delta Q^\star$ ensure that inverter power injections $P + \Delta P$, $Q + \Delta Q$ satisfy the feeder-head active- and reactive-power requirements, $P^\star_{\mathrm{grid}}$, $Q^\star_{\mathrm{grid}}$.

B. System State-space Model for Control Synthesis

Consider an AC power distribution network with nodes indexed in the set $\mathcal{N}$, with dispatchable inverters installed at nodes $\mathcal{I} \subseteq \mathcal{N}$. Collect nodal voltages, current injections, and complex-power injections in vectors $V \in \mathbb{C}^{|\mathcal{N}|}$, $I \in \mathbb{C}^{|\mathcal{N}|}$, and $S \in \mathbb{C}^{|\mathcal{N}|}$ respectively, and let $\theta \in \mathbb{T}^{|\mathcal{N}|}$ denote the vector of phase angles of the voltage phasors. In set $\mathcal{N}$, we denote the point of interconnection of the distribution network with the remainder of the bulk power system by node "grid".

Kirchoff's current law in matrix-vector form allows one to express $I = YV$, where Y is the network admittance matrix, and $S = \mathrm{diag}(V)I^*$. Application of the (multi-terminal) current-divider law yields the following expression for the current flowing in the line connecting the distribution network to the bulk grid [19]:

$$I_{\mathrm{grid}} = (\alpha^{\mathrm{T}}_{\mathrm{grid}} + \mathrm{j}\beta^{\mathrm{T}}_{\mathrm{grid}})I, \tag{1}$$

where $\alpha_{\mathrm{grid}} \in \mathbb{C}^{|\mathcal{N}|}$ and $\beta_{\mathrm{grid}} \in \mathbb{C}^{|\mathcal{N}|}$ depend on entries of the network-admittance matrix. Denote, by $S_{\mathrm{grid}} = P_{\mathrm{grid}} + \mathrm{j}Q_{\mathrm{grid}}$, the complex power flowing across line connecting the distribution feeder and transmission system, and by V_{grid} the voltage at the feeder head. We can further express the complex power flowing in the line connecting the distribution and transmission networks as $S_{\mathrm{grid}} = V_{\mathrm{grid}} I^*_{\mathrm{grid}}$. Substituting the expression for I_{grid} in (1) into the one for S_{grid} and using $I^* = \mathrm{diag}(V)^{-1}S$, we obtain

$$S_{\mathrm{grid}} = V_{\mathrm{grid}}(\alpha^{\mathrm{T}}_{\mathrm{grid}} - \mathrm{j}\beta^{\mathrm{T}}_{\mathrm{grid}})\mathrm{diag}(V)^{-1}S. \tag{2}$$

The real and imaginary parts of S_{grid} are given by

$$P_{\mathrm{grid}} = \varphi_{\mathrm{grid}} P + \kappa_{\mathrm{grid}} Q, \tag{3}$$

$$Q_{\mathrm{grid}} = \chi_{\mathrm{grid}} P + \lambda_{\mathrm{grid}} Q, \tag{4}$$

where the active- and reactive-power sensitivities are expressed as $\varphi_{\mathrm{grid}} = |V_{\mathrm{grid}}| u^{\mathrm{T}}_{\mathrm{grid}} \in \mathbb{R}^{1\times|\mathcal{N}|}$, $\kappa_{\mathrm{grid}} = -|V_{\mathrm{grid}}| v^{\mathrm{T}}_{\mathrm{grid}} \in \mathbb{R}^{1\times|\mathcal{N}|}$, $\chi_{\mathrm{grid}} = |V_{\mathrm{grid}}| v^{\mathrm{T}}_{\mathrm{grid}} \in \mathbb{R}^{1\times|\mathcal{N}|}$, $\lambda_{\mathrm{grid}} = |V_{\mathrm{grid}}| u^{\mathrm{T}}_{\mathrm{grid}} \in \mathbb{R}^{1\times|\mathcal{N}|}$, with $u_{\mathrm{grid}}, v_{\mathrm{grid}} \in \mathbb{R}^{|\mathcal{N}|}$ given by

$$u_{\mathrm{grid}} = \mathrm{diag}\left(\frac{\cos(\theta^{\mathrm{grid}})}{|V|}\right)\alpha_{\mathrm{grid}} + \mathrm{diag}\left(\frac{\sin(\theta^{\mathrm{grid}})}{|V|}\right)\beta_{\mathrm{grid}},$$

$$v_{\mathrm{grid}} = \mathrm{diag}\left(\frac{\sin(\theta^{\mathrm{grid}})}{|V|}\right)\alpha_{\mathrm{grid}} - \mathrm{diag}\left(\frac{\cos(\theta^{\mathrm{grid}})}{|V|}\right)\beta_{\mathrm{grid}}.$$

Above, $|V| \in \mathbb{R}^{|\mathcal{N}|}$ is the vector of nodal-voltage magnitudes; $\cos(x)$ and $\sin(x)$ denote vectors with entries equal to the cosine and sine of respective entries of x; $\mathrm{diag}(x/y)$ denotes a diagonal matrix with diagonal entries composed of ratios of entries of vectors x and y; and $\theta^{\mathrm{grid}} := \theta_{\mathrm{grid}}\mathbb{1}_{|\mathcal{N}|} - \theta \in \mathbb{T}^{|\mathcal{N}|}$ with θ_{grid} denoting the entry in θ corresponding to the feeder head and $\mathbb{1}_{|\mathcal{N}|}$ denoting a length-$|\mathcal{N}|$ vector with all entries equal to 1. (Readers are referred to [19] for more details.)

Suppose active- and reactive-power injections are sampled at $t = k\Delta t$, $k \in \mathbb{Z}$, where $\Delta t > 0$ is the time interval between consecutive samples. Consider small variations in nodal active- and reactive-power injections $\Delta P[k] = P[k+1] - P[k]$ and

$\Delta Q[k] = Q[k+1] - Q[k]$. Using (3), the effect of these small variations on P_{grid} and Q_{grid} can be approximated as

$$\begin{aligned} P_{\text{grid}}[k+1] \approx{}& \varphi_{\text{grid}}[k]\,(P[k] + \Delta P[k]) \\ &+ \kappa_{\text{grid}}[k]\,(Q[k] + \Delta Q[k])\,, \qquad (5) \\ Q_{\text{grid}}[k+1] \approx{}& \chi_{\text{grid}}[k]\,(P[k] + \Delta P[k]) \\ &+ \lambda_{\text{grid}}[k]\,(Q[k] + \Delta Q[k])\,. \qquad (6) \end{aligned}$$

In the above, φ_{grid}, κ_{grid}, χ_{grid}, and λ_{grid} are power sensitivities (denoted as "Sensitivities" in Fig. 1). These are central to the LQR controller that we will design in Section III. The approximations in (5)–(6) yield the following recurrence relations:

$$\begin{aligned} P_{\text{grid}}[k+1] ={}& P_{\text{grid}}[k] + \varphi_{\text{grid}}[k]\Delta P[k] \\ &+ \kappa_{\text{grid}}[k]\Delta Q[k] + w_P[k], \qquad (7) \\ Q_{\text{grid}}[k+1] ={}& Q_{\text{grid}}[k] + \chi_{\text{grid}}[k]\Delta P[k] \\ &+ \lambda_{\text{grid}}[k]\Delta Q[k] + w_Q[k], \qquad (8) \end{aligned}$$

where $w_P[k]$ and $w_Q[k]$ represent bounded external disturbances due to the linear approximation in (5)–(6) and model simplifications. We remark that in the above expression (and in all subsequent discussions), $\Delta P[k], \Delta Q[k] \in \mathbb{R}^{|\mathcal{I}|}$ contains only injections at the subset of nodes in the network with inverters, $\mathcal{I} \subseteq \mathcal{N}$. Accordingly, $\varphi_{\text{grid}}[k], \kappa_{\text{grid}}[k], \chi_{\text{grid}}[k], \lambda_{\text{grid}}[k] \in \mathbb{R}^{1\times|\mathcal{I}|}$. We proceed precariously with this slight abuse of notation.

III. Controller Design

Our goal is to track the active- and reactive-power grid injections, $P_{\text{grid}}[k]$ and $Q_{\text{grid}}[k]$, to some reference $P^\star_{\text{grid}}[k]$ and $Q^\star_{\text{grid}}[k]$ trajectories using inverter power injections, $\Delta P[k]$ and $\Delta Q[k]$, as control inputs. In this section, we propose to use an LQR controller to achieve optimal tracking of active and reactive power at the feeder head. We subsequently detail our implementation of the controller.

A. Linear-quadratic Regulator

Denote $\Delta\Sigma^\star[k] = [(\Delta P^\star[k])^{\mathrm{T}}, (\Delta Q^\star[k])^{\mathrm{T}}]^{\mathrm{T}} \in \mathbb{R}^{2|\mathcal{I}|}$, $w[k] = [w_P[k], w_Q[k]]^{\mathrm{T}}$, $\Sigma_{\text{grid}}[k] = [P_{\text{grid}}[k], Q_{\text{grid}}[k]]^{\mathrm{T}} \in \mathbb{R}^2$, $\Sigma^\star_{\text{grid}}[k] = [P^\star_{\text{grid}}[k], Q^\star_{\text{grid}}[k]]^{\mathrm{T}} \in \mathbb{R}^2$, and

$$\psi_{\text{grid}}[k] = \begin{bmatrix} \varphi_{\text{grid}}[k] & \kappa_{\text{grid}}[k] \\ \chi_{\text{grid}}[k] & \lambda_{\text{grid}}[k] \end{bmatrix} \in \mathbb{R}^{2\times 2|\mathcal{I}|}. \qquad (9)$$

The optimal LQR control feedback law is given by

$$\Delta\Sigma^\star[k] = -K\left(\Sigma_{\text{grid}}[k] - \Sigma^\star_{\text{grid}}[k]\right), \qquad (10)$$

where the feedback gain $K \in \mathbb{R}^{2|\mathcal{I}|\times 2}$ is designed in order to minimize the following quadratic cost function:

$$\begin{aligned} J = {}& \sum_{k=0}^{\infty} (\widehat{\Sigma}_{\text{grid}}[k] - \Sigma^\star_{\text{grid}}[k])^{\mathrm{T}} \Psi (\widehat{\Sigma}_{\text{grid}}[k] - \Sigma^\star_{\text{grid}}[k]) \\ &+ \sum_{k=0}^{\infty} (\Delta\Sigma^\star[k])^{\mathrm{T}} \Pi \Delta\Sigma^\star[k], \qquad (11) \end{aligned}$$

subject to the constraint

$$\widehat{\Sigma}_{\text{grid}}[k+1] = \widehat{\Sigma}_{\text{grid}}[k] + \psi_{\text{grid}}[k]\Delta\Sigma^\star[k], \qquad (12)$$

with initial condition $\widehat{\Sigma}[0] = \Sigma[0]$.

The constraint in (12) above is obtained from (7)–(8). In the cost function (11), positive definite $\Psi \in \mathbb{R}^{2\times 2}$ and $\Pi \in \mathbb{R}^{2|\mathcal{I}|\times 2|\mathcal{I}|}$ are performance-index weighing matrices. Namely, Ψ specifies the cost of feeder-head active power deviating away from its reference value, and Π embeds the cost of the control inputs, in our case, power injections from inverters. In accordance with standard LQR design, K is the optimal state-feedback gain, given by [20]

$$K = (\Pi + \psi^{\mathrm{T}}_{\text{grid}}[k] G \psi_{\text{grid}}[k])^{-1} \psi^{\mathrm{T}}_{\text{grid}}[k] G, \qquad (13)$$

where $G \in \mathbb{R}^{2\times 2}$ is the unique positive definite solution of the discrete algebraic Riccati equation (DARE) [20]

$$\Psi - G\psi_{\text{grid}}[k](\Pi + \psi^{\mathrm{T}}_{\text{grid}}[k] G \psi_{\text{grid}}[k])^{-1} \psi^{\mathrm{T}}_{\text{grid}}[k] G = 0. \qquad (14)$$

B. Implementation Details

At each time instant k, the LQR controller, which uses the system in (12), only requires measurements of active- and reactive-power injections at the feeder head collected in $\Sigma_{\text{grid}}[k]$ and provides actuation signals $\Delta\Sigma^\star[k]$ computed from (10). Simultaneously, the controller obtains updated sensitivities $\psi_{\text{grid}}[k]$ to compute actuation signals for the next time instant, $\Delta\Sigma^\star[k+1]$. It is worth emphasizing that the LQR optimal feedback controller is capable of tracking feeder head active- and reactive-power injections even in the face of imperfections such as errors arising from linear approximations in (5)–(6) and model simplifications.

IV. Numerical Case Studies

We focus on the problem of regulating the active and reactive power at the feeder head of the modified IEEE 37-bus distribution feeder shown in Fig. 2. The distribution network comprises 15 dispatchable inverters with five different power

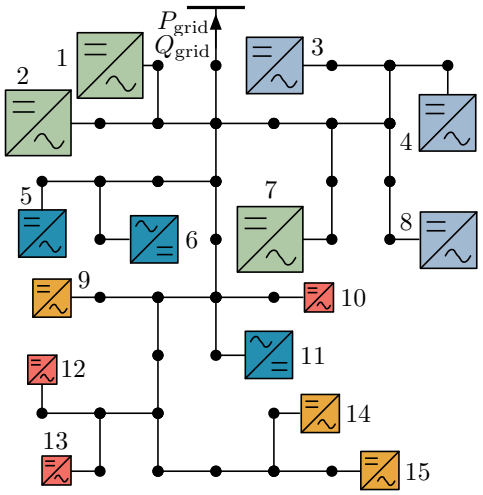

Fig. 2: Modified IEEE 37-bus network with 15 inverters. Color coding and size indicate identical power rating.

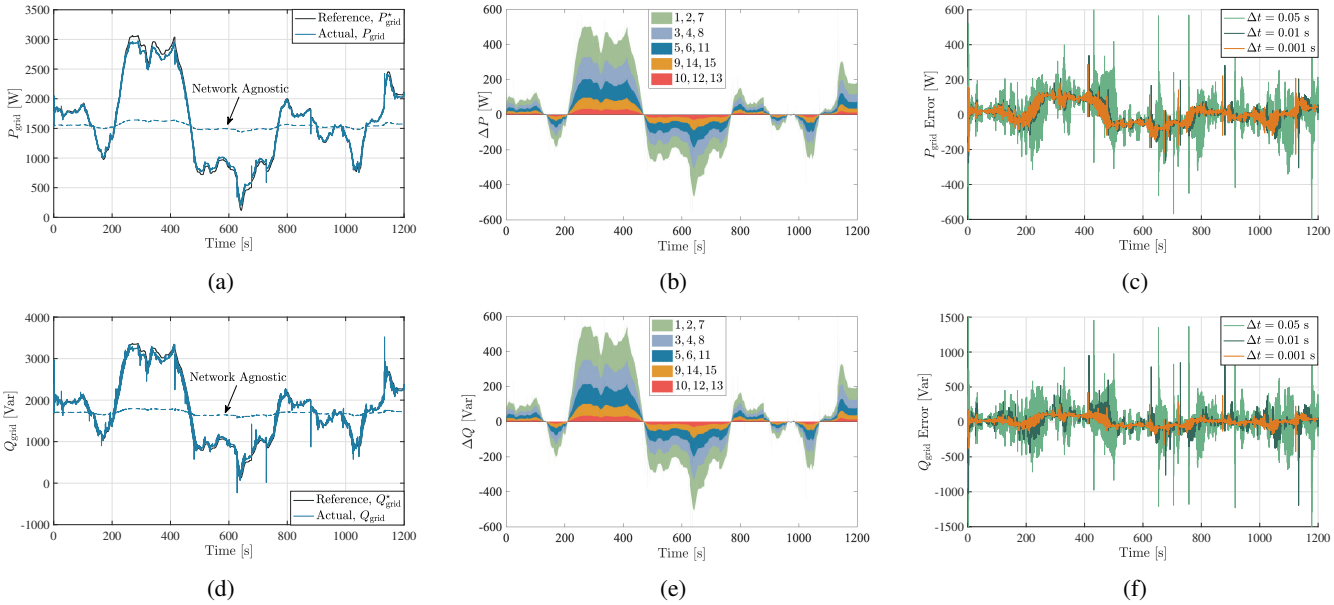

Fig. 3: Simulation results for the IEEE 37-bus distribution feeder: Proposed controller tracks the PJM RegD signal for both active- and reactive-power feeder head injections. (a),(d): Active- and reactive-power injections at the feeder head closely match desired trajectories. Network agnostic case (sensitivities assumed to be unity) demonstrates poor performance. (b), (e): Active- and reactive-power injections of inverters are in proportion to their capacities. (c), (f): Active- and reactive-power grid injection tracking accuracy for different sampling and dispatch rates.

ratings, which are indicated by colour and size in Fig. 2. For the regulation signal, without loss of generality, we choose the PJM regD trajectory for both active- and reactive-power tracking. We sample P_{grid} and Q_{grid} from the simulation periodically (with time intervals of, e.g., $\Delta t = 0.01\,\text{s}$ in Section IV-A) and collect them in Σ_{grid}. At each time step, we also recompute the nodal active- and reactive-power injection sensitivities ψ_{grid} from (9), using which, the optimal feedback gain K is computed using (13). Then, leveraging the recomputed sensitivities and feedback gain, the controller determines the optimal inverter injections $\Delta P^{\star}$ and $\Delta Q^{\star}$, which we collect in $\Delta\Sigma^{\star}$, using (10). Time-domain simulations of the test system in Fig. 2 acknowledge the nonlinear 15th-order inverter dynamics as described in Section II-A.

A. Benchmark Results

The PJM RegD signal is fed into the controller over a period of 20 minutes, where the reference setpoint changes every 1 s, which represents a more restrictive setting than the rate of 2 s required by PJM. Even so, the controller is able to track the reference feeder-head active- and reactive-power injections closely, as shown in Figs. 3a and 3d, respectively. For comparison, we also plot the feeder-head active- and reactive-power in the network-agnostic case when the LQR controller acts with all inverter active- and reactive-power injection sensitivities set to 1. Inverter power ratings are reflected in the controller via the weighing matrix Π in (11), where each diagonal entry is inversely proportional to the corresponding inverter capacity. Resulting inverter active- and reactive-power injections are proportional to capacity, as shown in Figs. 3b and 3e, respectively. The effectiveness of the proposed controller was quantitatively benchmarked against PJM's performance score (unitless between 0 and 1) that assesses the accuracy and precision with which a regulation resource provides regulation services [16]. The results shown in Figs. 3a and 3d represent a combined active- and reactive-power regulation performance score of 0.9998. As a point of comparison, a minimum score of 0.75 is required to take part in the PJM ancillary services market [16].

TABLE I: Overall controller performance score for different sampling and dispatch rates.

Time Interval [s]	Performance Score
0.05	0.9963
0.01	0.9998
0.001	0.9999

B. Effect of Sampling and Dispatch Rates

The accuracy of controller active- and reactive-power grid injection tracking can be improved by reducing the sampling and dispatch rates of inverter injections. Figures 3c and 3f show the active- and reactive-power tracking errors for various sampling and dispatch rates. We notice that the errors diminish for smaller time intervals between consecutive sampling and dispatch instants. The overall performance score (for both active- and reactive-power feeder injection tracking) with time intervals of $\Delta t = 0.05\,\text{s}$, $\Delta t = 0.01\,\text{s}$, and $\Delta t = 0.001\,\text{s}$ are reported in Table I.

V. Concluding Remarks & Future Work

In this paper, we proposed a method for regulating active- and reactive-power feeder injections in distribution networks. The main advantages of the proposed controller are that it

affords an intuitive method for tuning of design parameters and innately embeds network attributes via sensitivities of nodal power injections. The proposed controller time-domain dynamic performance was demonstrated using case studies involving the IEEE 37-bus distribution feeder test system. Compelling avenues for future work include extending the developed framework to incorporate a Kalman filter state estimator, measurement-based sensitivities, and voltage regulation at the feeder head.

REFERENCES

[1] C. Loutan and D. Hawkins, "Integration of renewable resources: Transmission and operating issues and recommendations for integrating renewable resources on the California ISO-controlled grid," tech. rep., North American Electric Reliability Corporation (NERC), Nov 2007.

[2] D. S. Callaway and I. A. Hiskens, "Achieving controllability of electric loads," *Proceedings of the IEEE*, vol. 99, pp. 184–199, Jan 2011.

[3] J. L. Mathieu, S. Koch, and D. S. Callaway, "State estimation and control of electric loads to manage real-time energy imbalance," *IEEE Transactions on Power Systems*, vol. 28, pp. 430–440, Feb 2013.

[4] Z. Ma, D. S. Callaway, and I. A. Hiskens, "Decentralized charging control of large populations of plug-in electric vehicles," *IEEE Transactions on Control Systems Technology*, vol. 21, pp. 67–78, Jan 2013.

[5] A. C. Kizilkale and R. P. Malhame, "Mean field based control of power system dispersed energy storage devices for peak load relief," in *52nd IEEE Conference on Decision and Control*, pp. 4971–4976, Dec 2013.

[6] Y. Lin, P. Barooah, S. Meyn, and T. Middelkoop, "Experimental evaluation of frequency regulation from commercial building HVAC systems," *IEEE Transactions on Smart Grid*, vol. 6, pp. 776–783, Mar 2015.

[7] S. S. Guggilam, C. Zhao, E. Dall'Anese, Y. C. Chen, and S. V. Dhople, "Optimizing DER participation in inertial and primary-frequency response," *IEEE Transactions on Power Systems*, vol. 33, pp. 5194–5205, Sep 2018.

[8] F. Teng, M. Aunedi, D. Pudjianto, and G. Strbac, "Benefits of Demand-Side Response in Providing Frequency Response Service in the Future GB Power System," *Frontiers in Energy Research*, vol. 3, p. 36, 2015.

[9] D. Fooladivanda, M. Zholbaryssov, and A. D. Dominguez-Garcia, "Control of networked distributed energy resources in grid-connected AC microgrids," *IEEE Transactions on Control of Network Systems*, vol. 5, pp. 1875–1886, Dec 2018.

[10] E. Dall'Anese, S. S. Guggilam, A. Simonetto, Y. C. Chen, and S. V. Dhople, "Optimal regulation of virtual power plants," *IEEE Transactions on Power Systems*, vol. 33, pp. 1868–1881, Mar 2018.

[11] S. P. Meyn, P. Barooah, A. Bušić, Y. Chen, and J. Ehren, "Ancillary service to the grid using intelligent deferrable loads," *IEEE Transactions on Automatic Control*, vol. 60, pp. 2847–2862, Nov 2015.

[12] A. Keane, L. F. Ochoa, E. Vittal, C. J. Dent, and G. P. Harrison, "Enhanced utilization of voltage control resources with distributed generation," *IEEE Transactions on Power Systems*, vol. 26, pp. 252–260, Feb 2011.

[13] B. Zhang, A. Y. S. Lam, A. D. Dominguez-Garcia, and D. Tse, "An optimal and distributed method for voltage regulation in power distribution systems," *IEEE Transactions on Power Systems*, vol. 30, pp. 1714–1726, Jul 2015.

[14] E. Dall'Anese, S. V. Dhople, and G. B. Giannakis, "Optimal dispatch of photovoltaic inverters in residential distribution systems," *IEEE Transactions on Sustainable Energy*, vol. 5, pp. 487–497, Apr 2014.

[15] K. Turitsyn, P. Sulc, S. Backhaus, and M. Chertkov, "Options for control of reactive power by distributed photovoltaic generators," *Proceedings of the IEEE*, vol. 99, pp. 1063–1073, Jun 2011.

[16] PJM, "PJM manual 12: Balancing operations," Feb 2019.

[17] A. Al-Digs, S. V. Dhople, and Y. C. Chen, "Measurement-based sparsity-promoting optimal control of line flows," *IEEE Transactions on Power Systems*, vol. 33, pp. 5628–5638, Sep 2018.

[18] V. Purba, S. V. Dhople, S. Jafarpour, F. Bullo, and B. B. Johnson, "Reduced-order structure-preserving model for parallel-connected three-phase grid-tied inverters," in *2017 IEEE 18th Workshop on Control and Modeling for Power Electronics (COMPEL)*, pp. 1–7, Jul 2017.

[19] Y. C. Chen and S. V. Dhople, "Power divider," *IEEE Transactions on Power Systems*, vol. 31, pp. 5135–5143, Nov 2016.

[20] M. Athans, "The role and use of the stochastic linear-quadratic-Gaussian problem in control system design," *IEEE Transactions on Automatic Control*, vol. 16, pp. 529–552, Dec 1971.